https://doi.org/10.15360/1813-9779-2025-3-2559

Skin Microcirculatory Parameters as Diagnostic Markers of Central and Cerebral Circulatory Disorders in Hemorrhagic Shock (An Experimental Study)

Ivan A. Ryzhkov[1]*, Nadezhda V. Golubova[1,2], Konstantin N. Lapin[1], Sergey N. Kalabushev[1], Viktor V. Dremin[2], Elena V. Potapova[2], Andrey V. Dunaev[2], Vladimir T. Dolgikh[1], Viktor V. Moroz[1]

[1] V. A. Negovsky Research Institute of General Reanimatology, Federal Research and Clinical Center of Intensive Care Medicine and Rehabilitology, 25 Petrovka Str., Bldg. 2, 107031 Moscow, Russia
[2] Orel State University, 95 Komsomolskaya Str., 302026 Orel, Russia

For citation: *Ivan A. Ryzhkov, Nadezhda V. Golubova, Konstantin N. Lapin, Sergey N. Kalabushev, Viktor V. Dremin, Elena V. Potapova, Andrey V. Dunaev, Vladimir T. Dolgikh, Viktor V. Moroz.* Skin Microcirculatory Parameters as Diagnostic Markers of Central and Cerebral Circulatory Disorders in Hemorrhagic Shock (An Experimental Study). *Obshchaya Reanimatologiya=General Reanimatology.* 2025; 21 (3). https://doi.org/10.15360/1813-9779-2025-3-2559 [In Russ. and Engl.]

***Correspondence to:** Ivan A. Ryzhkov, riamed21@gmail.com

Summary

The aim of the study was to evaluate the relationship between skin microcirculatory parameters and central and cerebral hemodynamic parameters during progressive blood loss.

Materials and Methods. A randomized, prospective, controlled in vivo experimental study was performed using male Wistar rats (250–350 g, *N*=23) divided into two groups: «hemorrhagic shock» (HS, *N*=13), with blood loss of 15% and subsequently 35% of estimated circulating blood volume (CBV), and «sham-operated» controls (SO, *N*=10). After combined anesthesia, femoral artery catheterization, and craniotomy, the following were measured at baseline (stage 1): mean arterial pressure (MAP), cortical cerebral perfusion ($LSCI_{brain}$), and skin perfusion in the hindlimb ($LSCI_{skin}$) using laser speckle contrast imaging (LSCI). These measurements were repeated after 15% CBV loss (stage 2) and 35% CBV loss (stage 3). Cerebral (CVC_{brain}=$LSCI_{brain}$/MAP) and cutaneous (CVC_{skin}=$LSCI_{skin}$/MAP) vascular conductance indices were calculated. At stage 3, parameters of post-occlusive reactive hyperemia (PORH) in hindlimb skin were additionally assessed. Statistical analysis was performed using STATISTICA 13.0 with non-parametric methods. Spearman's correlation coefficient (*R*) was used to assess associations between circulatory parameters.

Results. A 15% CBV loss led to a 26% reduction in $LSCI_{skin}$ (*P*=0.003 vs SO), with no significant change in $LSCI_{brain}$. With further blood loss and a 43% reduction in $LSCI_{skin}$ (*P*<0.001 vs SO), $LSCI_{brain}$ decreased by 14% (*P*<0.001 vs SO). These changes were accompanied by a sustained increase in CVC_{brain} (*P*<0.001 vs SO at stage 3), while CVC_{skin} remained unchanged throughout the experiment. In the HS group, blood loss led to a significant decrease in PORH amplitude (*P*=0.003 vs SO), while microvascular flow reserve increased (*P*=0.036 vs SO). Before blood loss, moderate positive correlations were found between $LSCI_{skin}$, CVC_{skin}, and CVC_{brain}. In HS, $LSCI_{brain}$ correlated with the degree of $LSCI_{skin}$ reduction (*R*=0.57, *P*=0.041), and skin microvascular flow reserve showed a strong positive correlation with arterial blood pH and base excess (BE) (*R*=0.84, *P*=0.001). The correlation between $LSCI_{skin}$ and MAP shifted from a moderate negative correlation at stage 1 to a strong positive correlation at stage 3.

Conclusion. Skin microcirculation parameters ($LSCI_{skin}$, CVC_{skin}, and PORH), as assessed by laser speckle contrast imaging, are promising diagnostic markers of central and cerebral hemodynamic impairment during progressive blood loss and warrant further validation.

Keywords: microcirculation; skin; brain; blood loss; laser speckle contrast imaging

Conflict of interest. The authors declare no conflict of interest.

Funding. This study was supported by the Russian Science Foundation (Project No. 24-25-00310).

Information about the authors:
Ivan A. Ryzhkov: AuthorID (RINTs): 781730, http://orcid.org/0000-0002-0631-5666
Nadezhda V. Golubova: AuthorID (RINTs): 1144542, http://orcid.org/0000-0001-5175-1486
Konstantin N. Lapin: AuthorID (RINTs): 1061143, http://orcid.org/0000-0002-7760-3526
Sergey N. Kalabushev: AuthorID (RINTs): 992594, http://orcid.org/0000-0001-7017-7897
Viktor V. Dremin: AuthorID (RINTs): 787806, http://orcid.org/0000-0001-6974-3505
Elena V. Potapova: AuthorID (RINTs): 240669, http://orcid.org/0000-0002-9227-6308
Andrey V. Dunaev: AuthorID (RINTs): 212404, http://orcid.org/0000-0003-4431-6288
Vladimir T. Dolgikh: AuthorID (RINTs): 540900, http://orcid.org/0000-0001-9034-4912
Viktor V. Moroz: AuthorID (RINTs): 168246

Introduction

Hemorrhagic shock (HS) is an acute circulatory failure resulting from significant blood loss. It is characterized by impaired tissue perfusion and oxygen delivery and carries a high risk for the development of multiple organ dysfunction [1]. The primary pathogenic trigger in acute hemorrhage and HS is profound hypovolemia, leading to a reduction in cardiac output, arterial hypotension, and peripheral hypoperfusion [1, 2]. Consequently, the assessment and timely correction of central hemodynamic parameters in the setting of hemorrhage are of critical importance in clinical practice [3].

However, it is the disruption of microcirculatory perfusion and tissue oxygenation that serves as a key mechanism underlying organ dysfunction in hemorrhagic and other forms of shock [4, 5]. Despite certain common features across organs, such as reduced perfused capillary density, heterogeneous microvascular flow, slowed capillary transit, increased blood viscosity, and increased endothelial permeability, microcirculatory disturbances exhibit organ-specific characteristics. These are largely determined by the variable intensity of vascular responses in different tissue beds triggered by hemorrhage and its associated pathophysiological processes [6].

During early blood loss, perfusion of vital organs such as the brain and heart may be temporarily preserved due to effective autoregulation and redistribution of blood flow (circulatory centralization). In contrast, perfusion of non-vital organs, including the skin, skeletal muscles, and abdominal viscera, is markedly reduced [5, 7]. However, as bleeding continues and shock progresses, these compensatory mechanisms are exhausted, leading to circulatory decompensation, global hypoperfusion, and hypoxic injury to even the most critical organs [6, 8, 9]. In cerebral circulatory decompensation during shock, not only the extent and rate of blood loss, but also systemic factors such as the patient's overall physiological condition, intracranial pressure, arterial blood gas composition, and the balance of the autonomic nervous system (between sympathetic and parasympathetic activity) play important pathophysiological roles [10].

Microcirculatory disturbances in internal organs play a central pathophysiological role in determining both the severity and prognosis of hemorrhage. However, most vital organs-such as the heart, brain, and lungs-are not readily accessible for direct visualization, creating methodological challenges in both experimental research and clinical evaluation of organ perfusion in shock and related conditions [4].

Experimental models of hemorrhage and hemorrhagic shock allow direct assessment of perfusion in internal organs through surgical access [11, 12]. On the other hand, superficial tissues such as skin and mucous membranes are readily accessible for non-invasive assessment of microcirculation and are often used as surrogate markers in studies of cardiovascular, endocrine and inflammatory disorders [13, 14].

Despite their relatively high tolerance to hypoxia, these tissues — as well as skeletal muscle and abdominal organs — often exhibit more pronounced microcirculatory impairment during hemorrhage and shock compared to the brain and myocardium [5].

In this context, the investigation of the relationship between cutaneous microcirculation and central and regional hemodynamic parameters is of great scientific and clinical importance. A key point of debate remains whether abnormalities in cutaneous blood flow detected by non-invasive methods accurately reflect disturbances in central or peripheral perfusion of internal organs [15–17]. This question is particularly critical in the context of critical care, where timely identification of circulatory compromise and organ dysfunction directly determines the scope and direction of intensive therapy [3, 18].

Experimental studies using laser Doppler flowmetry (LDF) have shown that the amplitude of microvascular flow oscillations (flowmotion) increases significantly in the early post-hemorrhagic period in both brain and skin, despite differences in the degree of hypoperfusion between these tissues [2]. Notably, even after reperfusion and apparent normalization of central hemodynamic parameters, microcirculatory function and cellular metabolism may remain impaired [19, 20].

In addition, several studies have highlighted the diagnostic and prognostic value of microcirculatory parameters in critical illness. The severity of microcirculatory dysfunction observed in experimental models or in patients with trauma and hemorrhagic shock has been shown to correlate with the extent of organ dysfunction and to be associated with adverse clinical outcomes [19, 21].

A variety of techniques have been developed to directly assess tissue perfusion and visualize the microvascular network. Among these, advanced *in vivo* microscopy, LDF and laser speckle contrast imaging (LSCI) are particularly noteworthy [13, 22]. LSCI is considered one of the most promising non-invasive modalities for clinical perfusion assessment, as it significantly reduces spatial heterogeneity in perfusion measurements. This method is increasingly being used to evaluate the cerebral microcirculation, both in animal models and in neurosurgical practice [23–25].

A critical ongoing challenge is the identification and validation of simple, clinically accessible diagnostic markers of impaired organ perfusion in shock. While LSCI has been used to detect microcirculatory

abnormalities in the skin of patients with cardiovascular, rheumatologic, endocrine, and dermatologic disorders [13], its use in clinical shock research remains limited. Only a handful of studies have used modern microcirculatory assessment techniques to investigate the relationship between cutaneous microcirculation and central hemodynamics or cerebral perfusion in hemorrhagic shock [16, 26], and the results have often been inconsistent.

The aim of the study was to evaluate the relationship between cutaneous microcirculatory parameters and central and cerebral hemodynamic parameters during progressive blood loss.

Material and Methods

This was a randomized, prospective, controlled, experimental study conducted in vivo in laboratory animals. Measures to reduce systematic bias included random assignment of animals to study groups to ensure comparability by body weight, and random sequencing of skin and cerebral blood flow measurements at each time point.

The study was conducted in accordance with national and international bioethical standards, including Directive 2010/63/EU. The experimental protocol was approved by the local ethics committee of the Federal Research and Clinical Center of Intensive Care Medicine and Rehabilitology (Protocol No. 1/24/2, dated April 24, 2024).

The study was conducted on male Wistar rats, aged 3–4 months, weighing 250–350 g. The initial sample size was *N*=30. The animals were randomly assigned to two groups:

- Group 1 (*N*=18): stepwise induction of blood loss leading to the development of hemorrhagic shock (HS group)
- Group 2 (*N*=12): sham-operated control group without blood loss (SO group).

A combined anesthetic protocol was used: tiletamine/zolazepam (Zoletil 100, Virbac, France) at 20 mg/kg and xylazine (Xylanit, NITA-FARM, Russia) at 5 mg/kg, both administered intraperitoneally. If a pain response indicated insufficient depth of anesthesia, an additional dose of Zoletil 100 (10 mg/kg, intraperitoneally) was administered.

For invasive arterial pressure monitoring and arterial blood sampling, the left femoral artery was catheterized with a polyethylene catheter (PE-50, OD 0.95 mm, ID 0.58 mm; SciCat, Russia). For local anesthesia of soft tissues and vessel walls, 1% lidocaine (not more than 0.4 mL per rat) was used. After catheter placement, the surgical wound was closed with temporary sutures. If necessary, the catheter was flushed with unfractionated heparin solution (5 IU/mL) in volumes of 0.1–0.2 mL.

Prior to craniotomy, the anesthetized and catheterized rat was positioned prone in a stereotaxic frame mounted on a temperature-controlled platform. The head was immobilized at three points - via the maxillary incisors and external auditory canals — using a stereotaxic device. Core body temperature was continuously monitored with a rectal probe, with target values maintained between 36.5 and 37.0°C. Animals breathed spontaneously throughout the procedure.

Craniotomy was performed in the left parietal region (corresponding to the vascular territory of the left middle cerebral artery and the sensorimotor cortex of the rat) according to a previously described protocol [27]. The coordinates for the center of the craniotomy were 4 mm caudal to bregma and 2.5 mm lateral to the midline suture. The diameter of the craniotomy was 2.5–3 mm. The dura mater and the inner bone layer (devoid of surface vessels) were left intact to maintain intracranial pressure and avoid injury to the pial vessels. A stabilization period of at least 15 minutes was allowed after craniotomy before measurements were started.

A fixed-volume hemorrhage model was used, with total blood loss set at 35% of the estimated circulating blood volume (CBV), corresponding to a class III hemorrhage (out of four) according to the ATLS classification [28]. The CBV (in mL) was calculated as 6.5% of the animal's body weight. Blood was collected using a sterile syringe in three consecutive draws (15% — 10% — 10% of total CBV), each lasting 2 min, with 8 min intervals between draws. The total bleeding time was 20–22 minutes. Reinfusion of blood was not performed. Animals were monitored for an additional 30 minutes after hemorrhage.

Electrocardiography (ECG) was recorded using needle electrodes integrated into the MouseMonitor S platform (INDUS Instruments, USA). The analog signal was transmitted to a PowerLab 16/35 data acquisition system (ADInstruments, Australia). Digitized ECG signals from three standard leads (I, II, III) were then analyzed using LabChart Pro 8 software (ADInstruments, Australia). Heart rate (HR) was calculated as the average beats per minute over a 5-minute recording period.

Arterial blood pressure (BP) was measured by connecting the femoral artery catheter to a Deltran DPT-100 pressure transducer (Utah Medical Products, USA) via a three-way stopcock and infusion line. The analog pressure signal was transmitted through the BP-100 amplifier (CWE Inc., USA) to the PowerLab 16/35 system. The digitized BP waveform was analyzed using LabChart Pro 8 software to determine mean arterial pressure (MAP) over the 5-minute measurement period.

For assessment of blood gas parameters and acid-base status, arterial blood samples (0.2 mL) were collected through the femoral catheter into 1.0 mL insulin syringes preflushed with a small volume of heparin. Blood gas analysis — including pH, pCO_2, pO_2, base excess (BE), bicarbonate (HCO_3^-),

arterial oxygen saturation (SaO_2), and lactate concentration — was performed using CG4+ reagent cartridges with the i-STAT 1 handheld analyzer (Abbott Point of Care Inc., USA).

Cerebral cortical and limb skin perfusion in rats was assessed using laser speckle contrast imaging (LSCI) with a custom-built setup. The measurement principle and technical specifications of this method have been described previously [27]. Speckle images were acquired from the left parietal region of the skull and the plantar surface of the right hind limb. The acquisition time for each anatomical region was 5 minutes (including a 2.5-minute acquisition between the first and second blood draws).

Monochromatic images were acquired and subsequently processed by pixel-wise calculation of spatiotemporal speckle contrast values over the entire field of view. The images were then color-coded using pseudocolor mapping according to the calculated LSCI perfusion values (defined as $1/K^2$), resulting in laser speckle perfusion maps (see Fig. 1). The derived signal was analyzed to quantify LSCI perfusion in skin ($LSCI_{skin}$) and brain cortex ($LSCI_{brain}$), expressed in arbitrary perfusion units (AU). The anatomical locations used for perfusion measurements are shown in Fig. 1.

Due to the limited field of view of the LSCI setup, sequential imaging of skin and cerebral perfusion was performed at each of the three experimental time points. To minimize systematic measurement bias, the order of imaging (skin followed by brain or vice versa) was randomized for each animal in both groups.

In addition to the mean LSCI perfusion values obtained at each stage of the experiment, cutaneous vascular conductance (CVC_{skin}) was calculated as $LSCI_{skin}$ divided by mean arterial pressure (CVC_{skin} = $LSCI_{skin}$ / MAP, AU/mmHg). This index allows standardization of perfusion relative to systemic blood pressure and serves as an indirect measure of vascular tone [13]. Similarly, cerebral vascular conductance (CVC_{brain} = $LSCI_{brain}$ / MAP) was calculated.

At the end of the experiment, a functional occlusion test was performed on the hind limb of the rat to assess post-occlusive reactive hyperemia (PORH). A pneumatic cuff from the non-invasive blood pressure monitoring system «Systola» (Neurobotics, Russia) was placed around the mid-calf level of the right hind limb and connected to an aneroid manometer. LSCI perfusion was recorded for 30 seconds at baseline (resting state). The cuff was then inflated to 200–220 mmHg and maintained at this pressure for an additional 30 seconds. After rapid cuff deflation, LSCI recording continued for an additional 60 seconds.

PORH parameters were assessed in the same skin area (plantar surface of the limb) used for the previous perfusion measurements. The following PORH variables were calculated:

- LSCI perfusion at rest with cuff in place ($LSCI_{rest}$, AU)

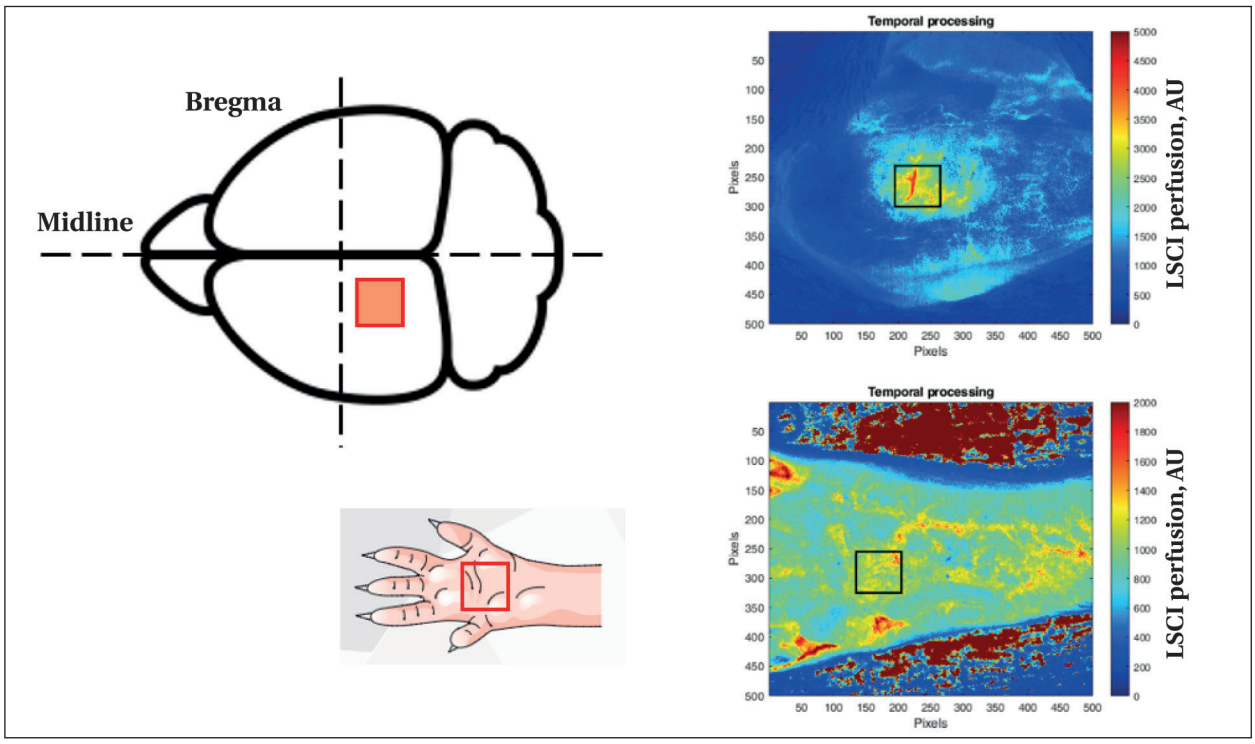

Fig. 1. Anatomical regions of the rat body where microcirculation was assessed using laser speckle contrast imaging (LSCI).
Note: Red squares indicate regions of the organ surface where perfusion was measured. To the right are examples of perfusion mapping in the cerebral cortex and skin of the hind limb.

• minimum LSCI values during occlusion, representing the biological zero ($LSCI_{occl}$, AU)

• peak reactive hyperemia, i.e. the maximum LSCI perfusion after cuff release ($LSCI_{max}$, AU)

• microvascular flow reserve, calculated as $LSCI_{max}$/ $LSCI_{rest}$

• peak cutaneous vascular conductance, calculated as $CVC_{max} = LSCI_{max}/MAP$ (AU/mmHg).

At the end of the procedure, animals were euthanized under general anesthesia (Zoletil 100 + xylazine) by intra-arterial injection of 2.0 mL 2% lidocaine. Death was confirmed by electrocardiographic criteria.

The main time points of the experiment at which physiological and laboratory parameters were recorded included:

1. Baseline — after induction of anesthesia, femoral artery catheterization, craniotomy, and a stabilization period.

2. Blood loss 15% of circulating blood volume (CBV) — measurements of the same physiologic parameters as at baseline (except arterial blood gas and acid-base balance) were performed during the interval between the first and second blood draws.

3. Blood loss 35% of CBV — the same physiological and laboratory parameters as at baseline were recorded 20 to 30 minutes after the end of the bleeding.

Measurements of central, cerebral, and cutaneous hemodynamics — including MAP, HR, and LSCI perfusion of the sensorimotor cortex and hind limb skin — were performed at all time points. Arterial blood gas (ABG) and acid-base balance (ABB) parameters and ECG recordings were obtained only at time points 1 (baseline) and 3 (blood loss 35%) (see Fig. 2).

The occlusion test on the rat hind limb was performed once at the end of the experiment, at the third time point, after LSCI measurements of cerebral and cutaneous perfusion had been completed.

In the sham-operated control group (SO), no blood loss was induced; however, all measurements were performed at the same time intervals as in the bleeding group.

The required sample size was estimated using StatMate 2.0 software (GraphPad Software, USA) based on data from a preliminary series of experiments. The calculation was performed taking into account the variability of the cerebral cortex speckle perfusion index (SD = 287 AU), an expected mortality rate of approximately 30% in the HS group, and a desired statistical power greater than 0.9.

Statistical analysis of the data obtained was performed using Statistica 13.0 software (StatSoft, USA). Because most variables did not follow a normal distribution (as assessed by the Shapiro–Wilk test), intergroup differences were analyzed using the Mann–Whitney *U* test. Within-group changes were assessed using the Friedman test, followed by pairwise comparisons using the Wilcoxon signed-rank test with Bonferroni correction.

Results are expressed as median and interquartile range *Me* ([25%; 75%]). Correlations between parameters were assessed using Spearman's rank

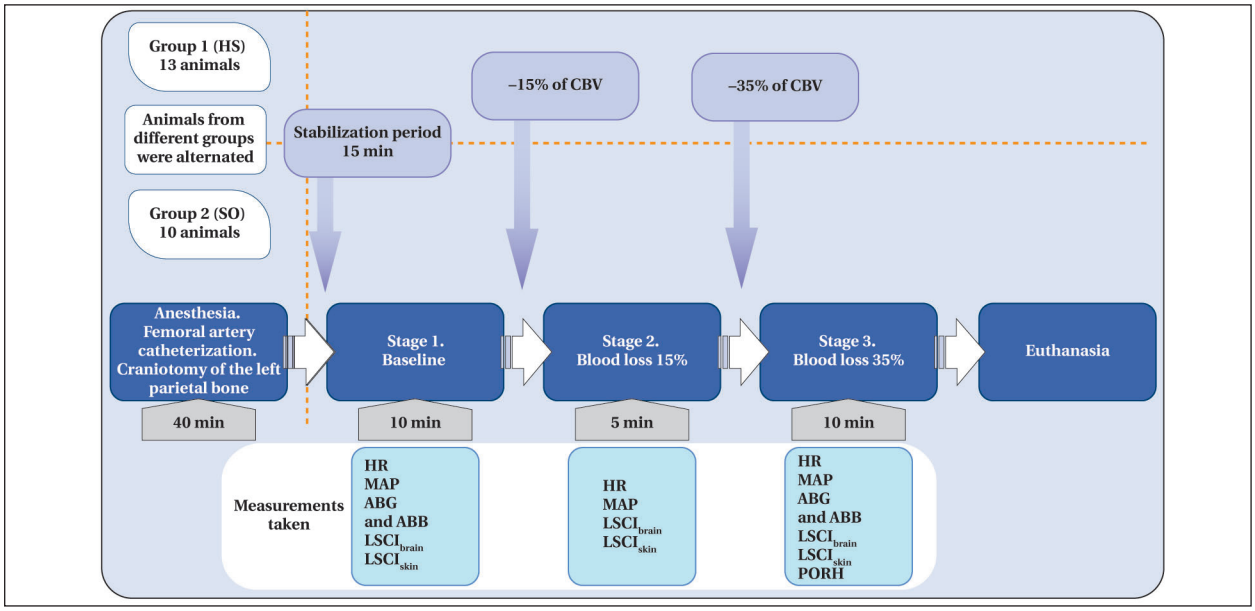

Fig. 2. Schematic representation of the experimental design

Note. During the experiments, 2 animals from the SO group and 5 animals from the HS group were excluded from the study according to predefined exclusion criteria (severe surgical complications, multiple significant protocol deviations). No deaths occurred in either group. Thus, 23 animals were included in the final analysis (SO, *N*=10; HS, *N*=13).

CBV — estimated circulating blood volume; HR — heart rate; MAP — mean arterial pressure; ABG — acid-base status; $LSCI_{brain}$ and $LSCI_{skin}$ — cerebral cortex and skin perfusion, respectively, measured by LSCI; PORH — post-occlusive reactive hyperemia.

correlation coefficient (R). A two-tailed $P<0.05$ was considered statistically significant.

Results

Postmortem examination of the animals' skulls (after euthanasia) revealed that the cranial window area was maximally thinned (⩽0.3 mm) but not perforated. None of the animals included in the analysis showed evidence of intracranial hemorrhage or other evidence of brain injury.

There were no significant differences in central and peripheral hemodynamic parameters between groups at baseline (Stage 1) ($P>0.05$, Mann–Whitney U test, Table 1). However, the total dose of anesthetic tiletamine/zolazepam was lower in the HS group compared to the SO group (40 [30; 40] vs. 53 [50; 55] mg/kg; $P=0.01$), as animals in the HS group required a lower maintenance dose after blood loss to achieve the same depth of anesthesia.

After 15% blood volume loss (stage 2), MAP in the HS group decreased by 26% from baseline and was significantly lower than in the SO group (Fig. 3, *a*). HR decreased by 16% in the HS group compared to baseline, but the difference between the groups for this parameter did not reach statistical significance (HS vs. SO, $P=0.057$) (Fig. 3, *b*).

The $LSCI_{skin}$ index in the HS group decreased by 26% compared to baseline in the same group as well as compared to the SO group (Fig. 4, *a*). $LSCI_{brain}$ in the HS group did not change significantly from stage 1 ($P=0.345$), but was 9% lower than in the SO group, where cerebral perfusion increased slightly (by 7%) relative to baseline in this group ($P=0.017$) (Fig. 4, *b*). In this context, cutaneous vascular conductance (CVC_{skin}) did not differ between the HS and SO groups ($P=0.702$) and remained unchanged from baseline in both groups (Fig. 4, *c*). Meanwhile, cerebral vascular conductance (CVC_{brain}) increased by 43% from baseline in the HS group ($P=0.002$) and was significantly higher than in the SO group (Fig. 4, *d*).

After 35% blood volume loss (stage 3), MAP in the HS group decreased by 32% from baseline and was significantly lower than in the SO group (Fig. 3, *a*). The HR at this stage was not significantly different

Table 1. Central and peripheral hemodynamic parameters in the study groups at Stage 1 (baseline).

Parameter	Values in groups		*P* value
	Group HS	Group SO	
MAP, mmHg	90 [79; 98]	94 [87; 95]	0.651
HR, bpm^{-1}	308 [289; 312]	303 [293; 325]	0.975
$LSCI_{skin}$, AU	1858 [1458; 2419]	1799 [1675; 1953]	0.976
$LSCI_{brain}$, AU	3407 [3066; 3618]	3657 [3291; 3878]	0.166
CVC_{skin}, AU/mmHg	20.3 [14.8; 25.9]	19.6 [18.3; 23.6]	0.917
CVC_{brain}, AU/mmHg	37.0 [29.6; 44.3]	41.3 [36.8; 41.4]	0.508

Note. MAP — mean arterial pressure; HR — heart rate; $LSCI_{skin}$ — laser speckle contrast imaging (LSCI)–derived skin perfusion; $LSCI_{brain}$ — LSCI-derived cerebral perfusion; CVC_{skin} — cutaneous vascular conductance; CVC_{brain} — cerebral vascular conductance. *P-values* represent between-group comparisons (Mann–Whitney U test).

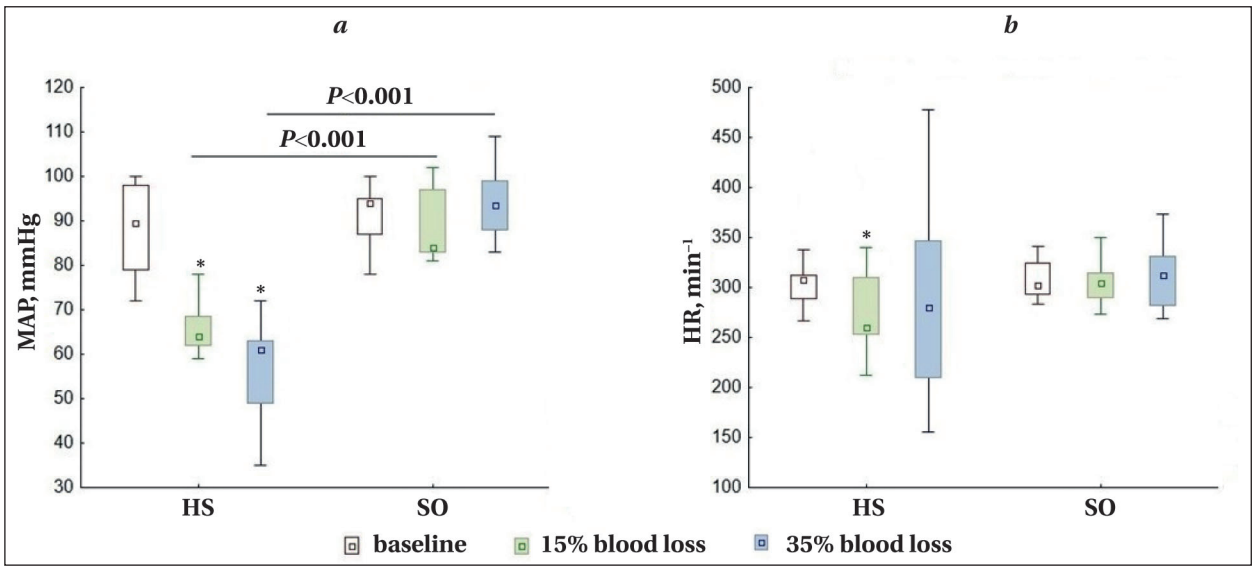

Fig. 3. Key parameters of central hemodynamics in rats at different experimental stages.
Note. *P* values indicate comparisons between groups (HS vs. SO) using the Mann–Whitney U test. * — $P<0.05$ vs. baseline (Wilcoxon test with Bonferroni correction).

from baseline (P=0.046 with Bonferroni correction) or from the SO group (P=0.257), although greater variability in HR values was noted within the HS group (Fig. 3, *b*).

Cutaneous perfusion ($LSCI_{skin}$) in the HS group decreased by 43% compared to both baseline (P=0.001) and SO (Fig. 4, *a*). The reduction in cerebral perfusion ($LSCI_{brain}$) in the HS group compared to stage 1 did not reach the significance level (P=0.116), but was 23% lower than in the SO group (Fig. 4, *b*). CVC_{skin} in the HS group after 35% blood loss did not change significantly from baseline and, as with moderate blood loss, did not differ between the HS and SO groups (P=0.257) (Fig. 4, *c*). In contrast, CVC_{brain} remained elevated by 37% from baseline (P=0.006) and was significantly higher than in the SO group (Fig. 4, *d*).

Characteristic speckle perfusion images of the skin and cerebral cortex obtained during the experiment are shown in Fig. 5.

The results of ABG and ABB measurements in laboratory animals are presented in Table 2.

At baseline, the groups differed only slightly in PaO_2 levels. Thirty minutes after blood loss, animals in the HS group showed changes in arterial blood gas and acid-base status typical of hemorrhagic shock: metabolic lactic acidosis (elevated blood lactate, decreased HCO_3 and BE levels, and decreased blood pH in some animals) with partial respiratory compensation (a trend toward hypocapnia in the

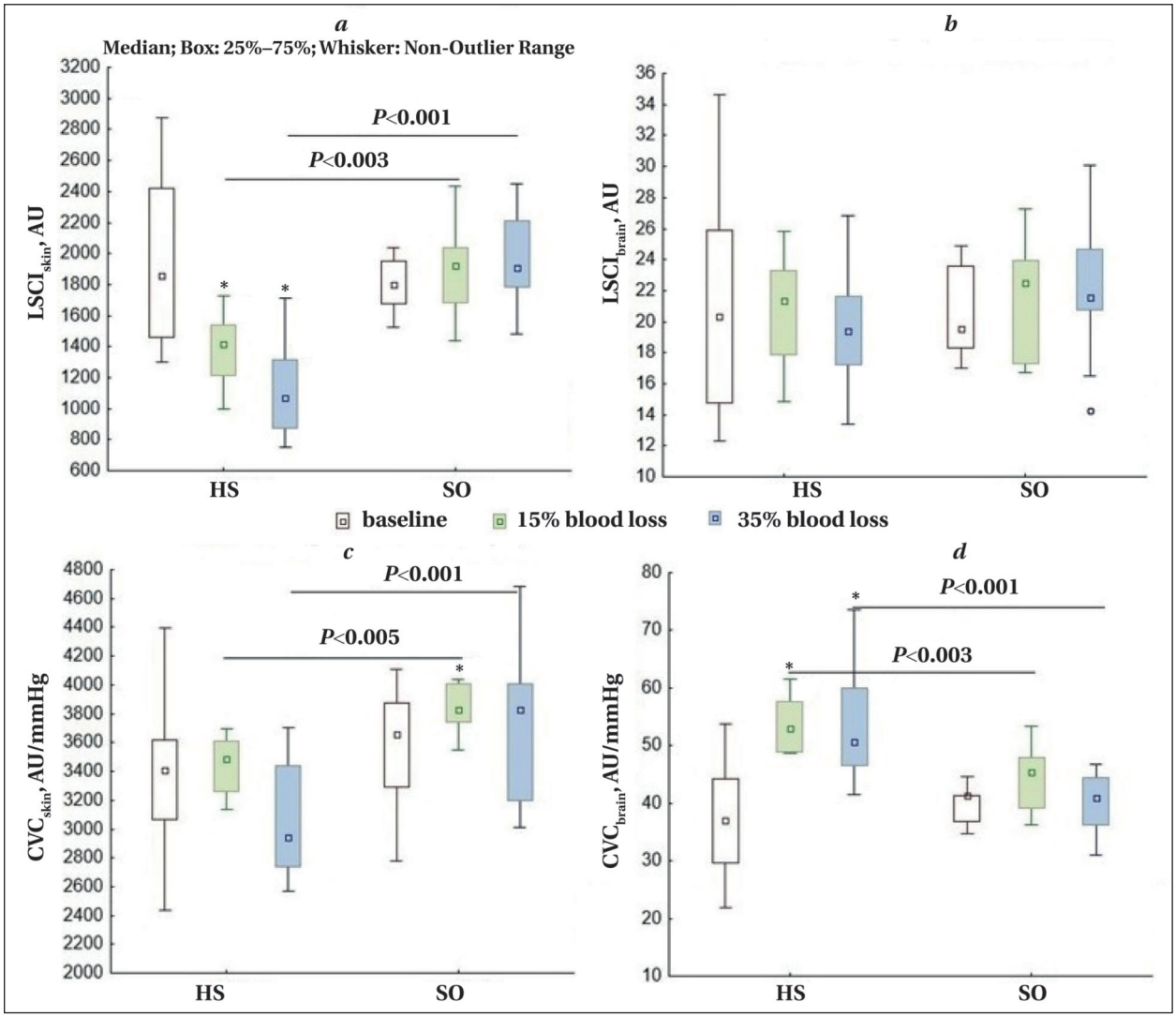

Fig. 4. Key parameters of skin and brain blood flow in rats at different experimental stages.
Note. The figure shows the changes in LSCI-derived skin perfusion (*a*), LSCI-derived brain perfusion (*b*), cutaneous vascular conductance (*c*), and cerebral vascular conductance (*d*) at baseline, after acute blood loss of 15% of the estimated CBV, and 30 min after acute blood loss of 35% CBV. *P* values indicate comparisons between groups (HS vs. SO) using the Mann–Whitney *U* test. * — P<0.05 vs. baseline (Wilcoxon test with Bonferroni correction).

HS group). Arterial blood oxygenation (PaO_2) increased significantly in the HS group at stage 3 compared with stage 1 (P=0.005, Wilcoxon test); however, no between-group differences in PaO_2 or SaO_2 were observed at stage 3 (Table 2).

At the end of stage 3, animals in both groups underwent the PORH test on the hind limb skin after a 30-second occlusion. The results of the occlusion test are shown in Fig. 6.

Correlation analysis was performed to identify biologically significant relationships between skin microcirculation parameters and central and cerebral circulation parameters. Since the groups of animals did not differ in the parameters studied at stage 1 (baseline), the correlation analysis at this stage was performed for the entire sample (N=23). Statistically significant correlations are shown in Fig. 7.

A separate correlation analysis was then performed in the HS group to identify biologically significant associations between skin microcirculation parameters (including PORH parameters) and central and cerebral circulation parameters at stage 3, when the animals developed hemorrhagic shock (Fig. 8).

Discussion

In this study, we investigated the relationship between changes in skin blood flow and cerebral and central circulation during moderate (15% of CBV) and severe (35% of CBV) acute blood loss. As the volume of blood loss increased, animals in the

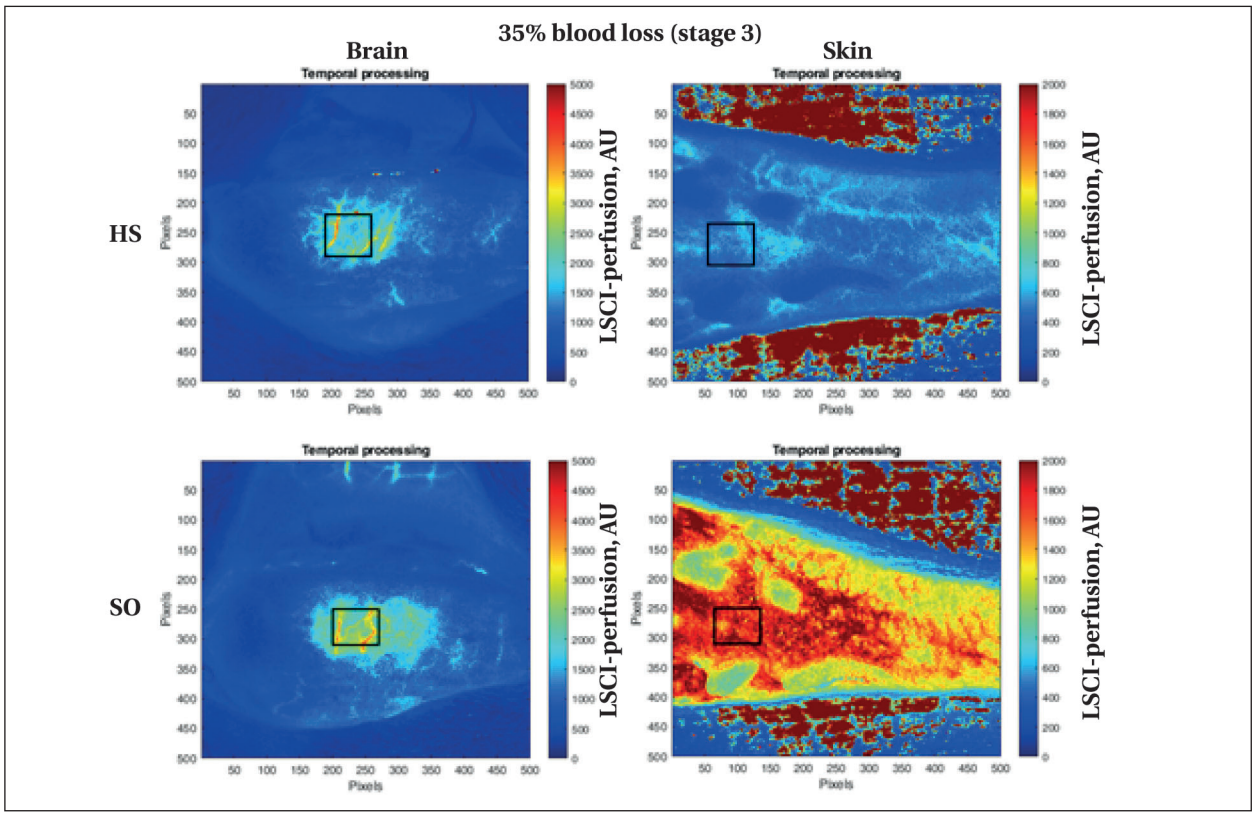

Fig. 5. Examples of speckle perfusion images of the brain and hind limb skin of a rat with 35% blood loss (HS group, top) and a control animal (SO group, bottom) without blood loss.

Table 2. Blood gas composition and acid-base status (ABG) of arterial blood in rats at baseline (Stage 1) and 30 minutes after acute blood loss of 35% blood volume (Stage 3).

Parameter	Values in groups at different stages					
	Stage 1 (baseline)			Stage 3 (blood loss of 35% CBV)		
	HS	SO	*P* value	HS	SO	*P* value
pH	7.40 [7.38; 7.45]	7.41 [7.41; 7.44]	0.257	7.38 [7.33; 7.40]	7.41 [7.39; 7.41]	0.131
$PaCO_2$, mmHg	36.3 [32.2; 38.3]	31.6 [28.6; 36.6]	0.208	27 [23.3; 30.1]	31.95 [29.2; 36.2]	**0.021**
PaO_2, mmHg	75 [70; 80]	83.5 [78; 85]	**0.042**	88 [86; 90]	79 [77; 83]	0.057
BE, mmol/L	–2 [–4; 0]	–2.5 [–4; –1]	0.648	–9 [–11; –6]	–3.5 [–6; –3]	**0.006**
HCO_3^-, mmol/L	21.8 [20.1; 23.0]	20.75 [19.7; 23.0]	0.522	15.1 [12.8; 18.8]	20.4 [18.1; 21.8]	**0.008**
SaO_2, %	95 [93; 96]	96.5 [96; 97]	0.67	97 [96; 97]	96 [95; 96]	0.148
Lactate, mmol/L	1.92 [1.20; 2.25]	1.37 [1.21; 1.73]	0.410	3.18 [2.01; 4.49]	1.76 [1.65; 2.18]	**0.008**

Note. Values with P<0.05 for comparisons between HS and SO groups (Mann–Whitney test) are highlighted in bold.

HS group consistently developed arterial hypotension. At the same time, heart rate variability increased in this group, with a tendency toward moderate bradycardia at stage 2. Tachycardia is known to be a normal compensatory response of the body to hemorrhage [5, 6]. The tendency towards bradycardia observed in this series of experiments can be explained by specific features of the hemorrhagic shock model: the use of combined anesthesia and rapid (within 2–3 minutes) blood removal at each stage of the study, i. e. a high bleeding rate. Both factors lead to a relative predominance of parasympathetic over sympathetic cardiac innervation, which delays the development of tachycardia during bleeding [29].

When measuring LSCI perfusion in the skin of the limb and the sensorimotor cortex of the brain during the post-hemorrhagic period, a consistent pattern was observed: a progressive decrease in skin perfusion with relative preservation of the cerebral microcirculation [7, 12]. To gain additional insight into the mechanisms underlying the reduction (or preservation) of tissue perfusion during blood loss, parameters of cutaneous and cerebral vascular conductance (CVC_{skin} and CVC_{brain}) were calculated. CVC, determined as the ratio of LSCI perfusion to MAP, reflects microvascular tone at the site of measurement and is often used in clinical studies to standardize assessment of skin perfusion under normal and pathological conditions [30]. Analysis of this parameter has shown that maintenance of cerebral microcirculation during blood loss occurs via an increase in cerebral CVC, representing a compensatory response to reduced cerebral perfusion pressure [10]. However, to our knowledge, no studies have used CVC parameters derived specifically from LSCI perfusion values to assess cerebral autoregulation during progressive hemorrhage.

During blood loss, cutaneous vascular conductance did not change significantly despite progressive skin hypoperfusion and other signs of evolving hemorrhagic shock (hypotension, metabolic lactic acidosis). This finding somewhat contradicts the widely accepted concept of «centralization of the circulation» during hypovolemia, which occurs due to activation of the sympathetic nervous system and increased vascular tone in the skin, skeletal muscles, and abdominal organs [3, 6]. However, important factors that also determine the response of the peripheral circulation to blood loss include anesthesia and the core body temperature [4]. The use of combined general anesthesia and maintenance of normal core body temperature during the experiments (to standardize the model) likely explains the absence of a vasoconstrictor response in the skin during bleeding. In addition, as with the observed relative bradycardia, the lack of peripheral vasoconstriction in response to severe blood loss (>30% of estimated blood volume) may be due to phase-dependent inhibition of sympathetic vascular control and impaired baroreflex-mediated blood pressure regulation [31]. This is supported by the shift in

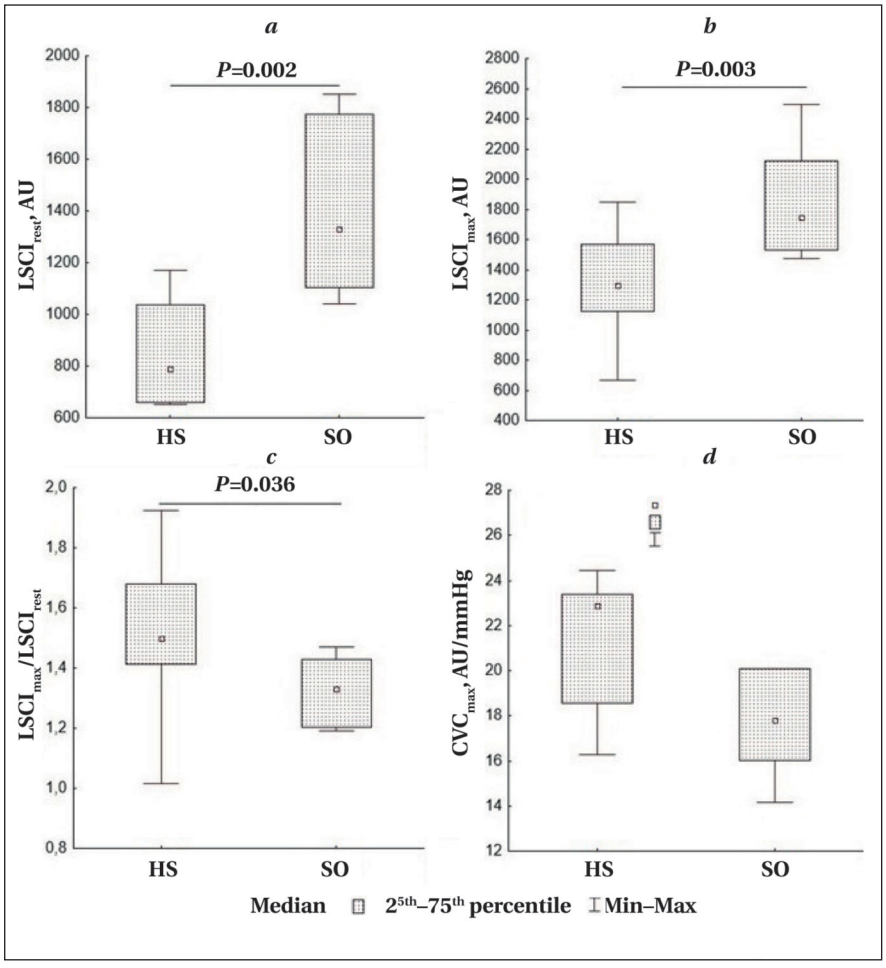

Fig. 6. Parameters of post-occlusive reactive hyperemia (PORH) in the skin of the hind limb of rats after acute blood loss of 35% of the total blood volume (stage 3).
Note. (*a*) Skin perfusion index ($LSCI_{rest}$) of the rat skin at rest with the cuff applied to the limb; (*b*) maximum skin perfusion index after cuff deflation ($LSCI_{max}$); AU — arbitrary units of perfusion; (*c*) skin microvascular blood flow reserve ($LSCI_{max}/LSCI_{rest}$); (*d*) cutaneous vascular conductance for maximum LSCI perfusion values (CVC_{max}).

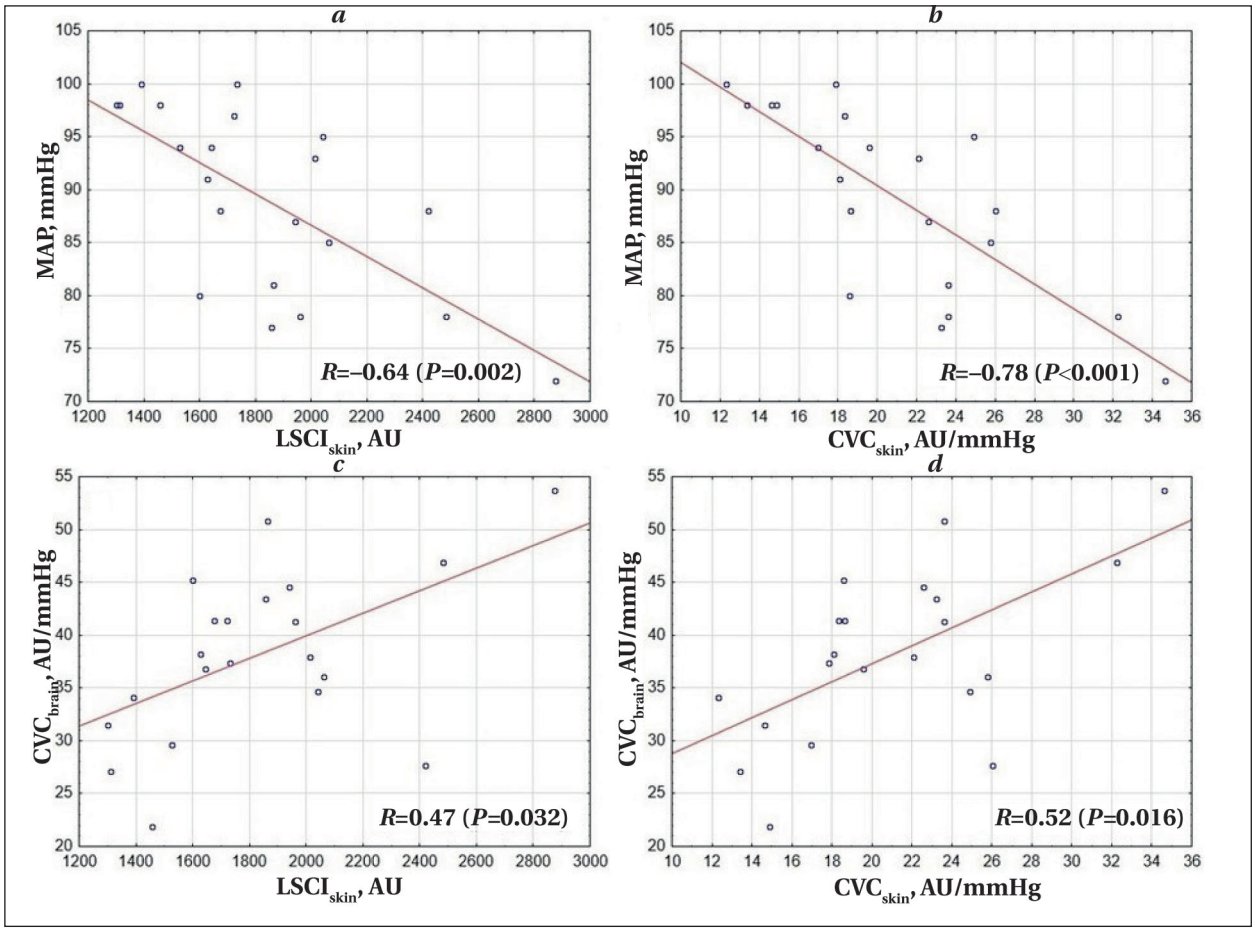

Fig. 7. Scatter plots showing the correlation between cutaneous circulation parameters and central and cerebral circulation parameters in rats (*N*=22) at stage 1 (before blood loss).
Note. MAP — mean arterial pressure, mm Hg; $LSCI_{skin}$ — LSCI perfusion of rat hind limb skin, AU; CVC_{skin} — cutaneous vascular conductance, AU/mm Hg; CVC_{brain} — cerebral vascular conductance, AU/mm Hg. Spearman's rank correlation coefficient (*R*) and corresponding *P* value are shown for each graph. One animal in the SH group was excluded from the analysis due to MAP measurement artifacts.

the correlation between $LSCI_{skin}$ and MAP from a moderately negative value (*R*=–0.64) at stage 1 to a strongly positive value (*R*=0.78) at stage 3. A strong correlation between CVC_{skin} and MAP (*R*=–0.78), present at stage 1, disappeared after the development of hemorrhagic shock.

Correlation analysis also revealed additional biologically and potentially clinically relevant associations between cutaneous and cerebral circulation parameters. At stage 1, a moderate positive correlation (*R*=0.52) was observed between CVC_{skin} and CVC_{brain}. At stage 3, in animals in hemorrhagic shock, cerebral perfusion was partially determined by the extent of skin perfusion reduction (*R*=0.57) — the greater the reduction in skin perfusion, the lower the cerebral blood flow. These findings highlight the potential diagnostic value of skin microcirculation parameters in assessing the severity of conditions such as intraoperative blood loss, particularly when patients are under general anesthesia and spontaneous hypothermia is intentionally prevented.

In this study, an occlusion test followed by analysis of PORH parameters was additionally used to assess skin microcirculation. Under conditions of hemorrhagic shock and pre-existing cutaneous hypoperfusion, a reduction in peak reactive hyperemia and a slight increase in microvascular flow reserve were observed. These findings are consistent with those of a previous experimental study [32] in which PORH was evaluated in rat skin during blood loss using LDF with an occlusion duration of 3 minutes (compared to 30 seconds in our study). They are also consistent with clinical observations showing a marked reduction in PORH in patients with severe blood loss as measured by infrared thermography of the fingers [16].

However, study [32] also reported an increase in peak vascular conductance (CVC_{max}) during the occlusion test in the setting of hemorrhagic shock. In contrast, in our study, the increase in this PORH parameter compared to the control group did not reach statistical significance.

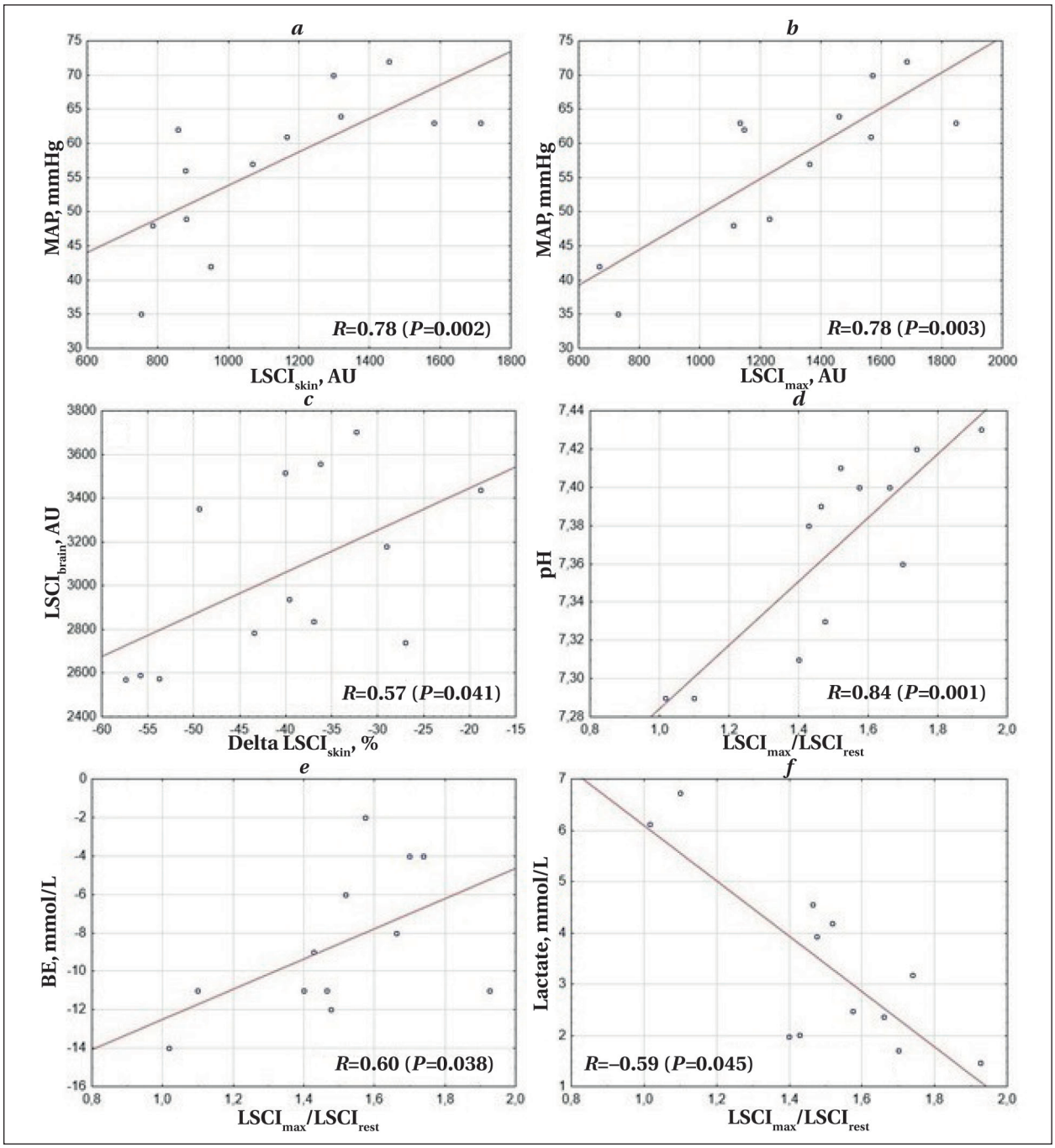

Fig. 8. Scatter plots illustrating the correlation between cutaneous microcirculation parameters and central and cerebral circulation parameters in HS group rats (*N*=12) at stage 3 (after 35% total blood volume loss).
Note. MAP — mean arterial pressure; $LSCI_{skin}$ — LSCI perfusion of rat hind limb skin, AU; $LSCI_{brain}$ — LSCI perfusion of rat cerebral cortex, AU; Delta $LSCI_{skin}$ — relative decrease in LSCI skin perfusion of rat hind limb after 35% blood loss, expressed as a percentage of baseline; $LSCI_{max}$ — maximum LSCI skin perfusion of the rat hind limb after cuff release during the occlusion test, AU; $LSCI_{max}/LSCI_{rest}$ — skin microvascular flow reserve, calculated as the ratio of $LSCI_{max}$ to baseline skin perfusion before vascular occlusion ($LSCI_{rest}$); BE and Lactate — base excess and blood lactate level in arterial blood, mmol/L, respectively. Spearman's rank correlation coefficient (*R*) and corresponding *P* values are shown for each graph. One animal in the HS group was excluded from the analysis due to artifacts in the MAP measurement.

Interestingly, correlation analysis revealed a positive association between cutaneous microvascular flow reserve (expressed as $LSCI_{max}/LSCI_{rest}$ ratio) and both arterial blood pH (*R*=0.84) and base excess (*R*=0.60), and a negative association with blood lactate level (*R*=–0.59). These associations were observed only during the development of hemorrhagic shock. Thus, low values of microvascular

flow reserve during blood loss may indicate the onset of decompensated lactic acidosis, which may have diagnostic value under certain conditions.

This study has several limitations. Cardiac output and total peripheral vascular resistance, important integrative parameters of central hemodynamics, could not be measured during the experiment. Their inclusion would have further improved the understanding of the causal relationships between central and peripheral circulatory changes. In addition, although the LSCI method provides a reliable assessment of perfusion changes over a relatively large area of tissue, it only captures perfusion in superficial layers (up to 0.5–1 mm depth). This limitation precludes the evaluation of microcirculatory changes in deeper tissue regions.

Further validation of skin microcirculatory parameters is warranted to establish their utility not only as diagnostic markers of impaired organ perfusion in hemorrhagic and other forms of shock, but also as prognostic indicators of outcome and therapeutic response in the critical care setting.

Conclusion

Under general anesthesia and normothermia, acute blood loss induces progressive cutaneous hypoperfusion with only minimal impairment of sensorimotor cortical perfusion. These changes are associated with a sustained increase in cerebral vascular conductance, while skin vascular conductance remains unchanged. Hemorrhagic shock is characterized by a reduced amplitude of post-occlusive reactive hyperemia. Before blood loss, moderate positive correlations were observed between cutaneous microcirculatory parameters (LSCI perfusion and cutaneous vascular conductance) and cerebral vascular conductance. In hemorrhagic shock, LSCI cortical perfusion correlates with the severity of skin hypoperfusion (R=0.57; P=0.041), and skin microvascular flow reserve correlates strongly with arterial pH (R=0.84; P=0.001). These findings support the potential of skin microcirculatory metrics as noninvasive indicators of central and cerebral hemodynamic compromise during progressive hemorrhage and hemorrhagic shock. Further studies are needed to validate their diagnostic and prognostic value in the critical care setting.

References

1. *Cannon J. W.* Hemorrhagic shock. *N Engl J Med.* 2018; 378 (19): 1852–1853. DOI: 10.1056/NEJMc1802361. PMID: 29742379
2. *Мороз В. В., Рыжков И. А.* Острая кровопотеря: регионарный кровоток и микроциркуляция (Обзор, Часть II). *Общая реаниматология.* 2016; 12 (5): 65–94. *Moroz V. V., Ryzhkov I. A.* Acute blood loss: regional blood flow and microcirculation (Review, Part II). *General Reanimatology = Obshchaya Reanimatologiya* 2016; 12 (5): 65–94. (in Russ.&Eng.). DOI: 10.15360/1813-9779-2016-5-65-94.
3. *Григорьев Е. В., Лебединский К. М., Щеголев А. В., Бобовник С. В., Буланов А. Ю., Заболотских И. Б., Синьков С. В., с соавт.* Реанимация и интенсивная терапия при острой массивной кровопотере у взрослых пациентов. *Анестезиология и реаниматология.* 2020; (1): 5–24. *Grigoriev E. V., Lebedinsky K. M., Shchegolev A. V., Bobovnik S. V., Bulanov A. Yu., Zabolotskikh I. B., Sinkov S. V., et al.* Resuscitation and intensive care in acute massive blood loss in adults (clinical guidelines). *Russian Journal of Anaesthesiology and Reanimatology = Anesteziologiya i Reanimatologiya.* 2020; (1): 5–24. (in Russ.). DOI: 10.17116/anaesthesiology20200115.
4. *Filho I. T.* Hemorrhagic shock and the microvasculature. *Compr Physiol.* 2017; 8 (1): 61–101. DOI: 10.1002/cphy.c170006. PMID: 29357125.
5. *Harrois A., Tanaka S., Duranteau J.* The microcirculation in hemorrhagic shock. Annual Update in Intensive Care and Emergency Medicine. 2013: 277–289. DOI: 10.1007/978-3-642-35109-9_22.
6. *Мороз В. В., Рыжков И. А.* Острая кровопотеря: регионарный кровоток и микроциркуляция (Обзор, Часть I). *Общая реаниматология.* 2016; 12 (2): 66–89. *Moroz V. V., Ryzhkov I. A.* Acute blood loss: regional blood flow and microcirculation (Review, Part I). *General Reanimatology = Obshchaya Reanimatologiya* 2016; 12 (2): 66–89. (in Russ.&Eng.). DOI: 10.15360/1813-9779-2016-2-66-89.
7. *Wan Z., Sun S., Ristagno G., Weil M. H., Tang W.* The cerebral microcirculation is protected during experimental hemorrhagic shock. *Crit Care Med.* 2010; 38 (3): 928–932. DOI: 10.1097/CCM.0b013e3181cd100c. PMID: 20068466.
8. *Cavus E., Meybohm P., Doerges V., Hugo H. H., Steinfath M., Nordstroem J., Scholz J., et al.* Cerebral effects of three resuscitation protocols in uncontrolled haemorrhagic shock: a randomised controlled experimental study. *Resuscitation.* 2009; 80 (5): 567–572. DOI: 10.1016/j.resuscitation.2009.01.013. PMID: 19217706.
9. *Рева В. А., Самакаева А. Р., Шелухин Д. А., Орлов С. В., Потемкин В. Д., Булгин Д. В., Грачева Г. Ю., с соавт.* Экстренная сверхглубокая гипотермия при остановке сердца, индуцированной кровопотерей (экспериментальное исследование на обезьянах). Общая реаниматология. 2025; 21 (1): 62–74. *Reva V. A., Samakaeva A. R., Shelukhin D. A., Orlov S. V., Potemkin V. D., Bulgin D. V., Gracheva G. Y., et al.* Emergency ultra-deep hypothermia in cardiac arrest induced by blood loss (experimental study on nonhuman primates). *General Reanimatology = Obshchaya Reanimatologiya.* 2025; 21 (1): 62–74. (in Russ.&Eng.). DOI: 10.15360/1813-9779-2025-1-62-74.
10. *Rickards C. A.* Cerebral blood-flow regulation during hemorrhage. *Compr Physiol.* 2015; 5 (4): 1585–1621. DOI: 10.1002/cphy.c140058. PMID: 26426461.
11. *Tonnesen J, Pryds A., Larsen E. H., Paulson O. B., Hauerberg J., Knudsen G. M.* Laser doppler flowmetry is valid for measurement of cerebral blood flow autoregulation lower limit in rats. *Exp Physiol.* 2005; 90 (3): 349–355. DOI: 10.1113/expphysiol.2004.029512. PMID: 15653714.
12. *Рыжков И. А., Заржецкий Ю. В., Новодержкина И. С.* Сравнительные аспекты регуляции кожной и мозговой микроциркуляции при острой кровопотере. *Общая реаниматология.* 2017; 13 (6): 18–27. *Ryzhkov I. A., Zarzhetsky Yu. V., Novoderzhkina I. S.* Comparative aspects of the regulation of cutaneous and cerebral microcirculation during acute blood loss. *General Reanimatology = Obshchaya Reanimatologiya.* 2017; 13 (6): 18–27. (in Russ.&Eng.). DOI: 10.15360/1813-9779-2017-6-18-27.
13. *Cracowski J., Roustit M.* Current methods to assess human cutaneous blood flow: an updated focus on laser-based-techniques. *Microcirculation.* 2016; 23 (5): 337–44. DOI: 10.1111/micc.12257. PMID: 26607042.
14. *Потапова Е. В., Михайлова М. А., Королева А. К., Ставцев Д. Д., Дремин В. В., Дунаев А. В., Якушкина Н. Ю., с соавт.* Мультипараметрический подход к оценке кожной микроциркуляции у пациентов дерматологического профиля (на примере псориаза). Физиол человека. 2021; 47 (6): 33–42. *Potapova E. V., Mikhailova M. A., Koroleva A. K., Stavtsev D. D., Dremin B. B., Dunaev A. V., Yakushkina N. Y., et al.* A multiparametric approach to assessing skin microcirculation in dermatological patients (using psoriasis as an

example). *Human physiology = Physiologiya Cheloveka*. 2021; 47 (6): 33–42. (in Russ.). DOI: 10.31857/S013116462105009X.
15. *Holowatz L. A., Thompson-Torgerson C. S., Kenney W. L.* The human cutaneous circulation as a model of generalized microvascular function. *J Appl Physiol (1985)*. 2008; 105 (1): 370–372. DOI: 10.1152/japplphysiol.00858.2007. PMID: 17932300.
16. *Ураков А. Л., Касаткин А. А., Уракова Н. А., Дементьев В. Б.* Инфракрасная термография пальцев рук человека как метод оценки адаптации регионарного кровообращения к кровопотере. *Регионарное кровообращение и микроциркуляция*. 2016; 15 (3): 24–29. *Urakov A. L., Kasatkin A. A., Urakova N. A., Dement'ev V. B.* Infrared thermography of human fingers as a method for assessing regional circulation adaptation to blood loss. *Regional Blood Circulation and Microcirculation = Regionarnoye Krovoobrashcheniye i Mikrocirkulyatsiya*. 2016; 15 (3): 24–29. (in Russ.). DOI: 10.24884/1682-6655-2016-15-3-24-29.
17. *Танканаг А. В.* Методы вейвлет-анализа в комплексном подходе к исследованию кожной микрогемодинамики как единицы сердечно-сосудистой системы. *Регионарное кровообращение и микроциркуляция*. 2018; 17 (3): 33–41. *Tankanag A. V.* Wavelet analysis methods in the comprehensive study approach of skin microhemodynamics as a cardiovascular unit. *Regional Blood Circulation and Microcirculation = Regionarnoye Krovoobrashcheniye i Mikrocirkulyatsiya*. 2018; 17 (3): 33–41. (in Russ.). DOI: 10.24884/1682-6655-2018-17-3-33-41.
18. *Остапченко Д. А., Гутников А. И., Давыдова Л. А.* Современные подходы к терапии травматического шока (обзор). *Общая реаниматология*. 2021; 17 (4): 65–76. *Ostapchenko D. A., Gutnikov A. I., Davydova L. A.* Current approaches to the treatment of traumatic shock (review). *General Reanimatology = Obshchaya Reanimatologiya*. 2021; 17 (4): 65–76. (in Russ.&Eng.). DOI: 10.15360/1813-9779-2021-4-65-76.
19. *Kerger H., Waschke K. F., Ackern K. V., Tsai A. G., Intaglietta M.* Systemic and microcirculatory effects of autologous whole blood resuscitation in severe hemorrhagic shock. *Am J Physiol*. 1999; 276 (6): H2035–43. DOI: 10.1152/ajpheart.1999.276.6.H2035. PMID: 10362685.
20. *González R., Urbano J., López J., Solana M. J., Botrán M., García A., Fernández S. N., et al.* Microcirculatory alterations during haemorrhagic shock and after resuscitation in a paediatric animal model. *Injury*. 2016; 47 (2): 335–341. DOI: 10.1016/j.injury.2015.10.075. PMID: 26612478.
21. *Tachon G., Harrois A., Tanaka S., Kato H., Huet O., Pottecher J., Vicaut E., et al.* Microcirculatory alterations in traumatic hemorrhagic shock. *Crit Care Med*. 2014; 42 (6): 1433–1441. DOI: 10.1097/CCM.0000000000000223. PMID: 24561562.
22. *Крупаткин А. И., Сидоров В. В.* Функциональная диагностика состояния микроциркуляторно-тканевых систем: Колебания, информация, нелинейность (Руководство для врачей). М: Книжный дом «ЛИБРИКОМ»; 2013: 496. *Krupatkin A. I., Sidorov V. V.* Functional diagnostics of microcirculatory and tissue systems: Fluctuations, information, nonlinearity (A manual for doctors). Moscow: LIBRIKOM Book House; 2013. 496. (in Russ.).
23. *Dunn A. K.* Laser speckle contrast imaging of cerebral blood flow. *Ann Biomed Eng*. 2012; 40 (2): 367–377. DOI: 10.1007/s10439-011-0469-0. PMID: 22109805.
24. *Piavchenko G., Kozlov I., Dremin V., Stavtsev D., Seryogina E., Kandurova K., Shupletsov V., et al.* Impairments of cerebral blood flow microcirculation in rats brought on by cardiac cessation and respiratory arrest. *J Biophotonics*. 2021; 14 (12): e202100216. DOI: 10.1002/jbio.202100216. PMID: 34534405.
25. *Golubova N., Potapova E., Seryogina E., Dremin V.* Time–frequency analysis of laser speckle contrast for transcranial assessment of cerebral blood flow. *Biomedical Signal Processing and Control*. 2023; 85: 104969. DOI: 10.1016/j.bspc.2023.104969.
26. *Ziebart A., Möllmann C., Garcia-Bardon A., Kamuf J., Schäfer M., Thomas R., Hartmann E. K.* Effect of gelatin-polysuccinat on cerebral oxygenation and microcirculation in a porcine haemorrhagic shock model. *Scand J Trauma Resusc Emerg Med*. 2018; 26 (1): 15. DOI: 10.1186/s13049-018-0477-2. PMID: 29426350.
27. *Golubova N., Ryzhkov I., Lapin K., Seryogina E., Dunaev A., Dremin V., Potapova E.* Effect of thinned-skull cranial window on monitoring cerebral blood flow using laser speckle contrast imaging. *IEEE J Select Topics Quantum Electron*. 2025; 31 (4): 1–8. DOI: 10.1109/JSTQE.2025.3533950
28. *Vishwanathan K., Chhajwani S., Gupta A., Vaishya R.* Evaluation and management of haemorrhagic shock in polytrauma: clinical practice guidelines. *J Clin Orthop Trauma*. 2020; 13: 106–15. DOI: 10.1016/j.jcot.2020.12.003. PMID: 33680808.
29. *Secher N. H., Van Lieshout J. J.* Heart rate during haemorrhage: time for reappraisal. *J Physiol*.

2010; 588 (Pt 1): 19.
DOI: 10.1113/jphysiol.2009.184499.
PMID: 20045902.

30. *Tew G. A., Klonizakis M., Crank H., Briers J. D., Hodges G. J.* Comparison of laser speckle contrast imaging with laser Doppler for assessing microvascular function. *Microvasc Res.* 2011; 82 (3): 326–32.
DOI: 10.1016/j.mvr.2011.07.007.
PMID: 21803051.
31. *Schadt J. C., Ludbrook J.* Hemodynamic and neurohumoral responses to acute hypovolemia in conscious mammals. *Am J Physiol.* 1991; 260 (2 Pt 2): H305–18.
DOI: 10.1152/ajpheart.1991.260.2.H305.
PMID: 1671735.
32. *Dubensky A., Ryzhkov I., Tsokolaeva Z;, Lapin K., Kalabushev S., Varnakova L., Dolgikh V.* Post-occlusive reactive hyperemia variables can be used to diagnose vascular dysfunction in hemorrhagic shock. *Microvasc Res.* 2024; 152: 104647.
DOI: 10.1016/j.mvr.2023.104647.
PMID: 38092223.

Received 11.03.2025
Accepted 22.04.2024
Online first 23.04.2025